Applied Catalysis B: Environmental 84 (2008) 176–184

Contents lists available at ScienceDirect

Applied Catalysis B: Environmental

journal homepage: www.elsevier.com/locate/apcatb

Total oxidation of propane using nanocrystalline cobalt oxide and supported cobalt oxide catalysts

Benjamin Solsona [a,*], Thomas E. Davies [b], Tomas Garcia [c], Isabel Vázquez [a], Ana Dejoz [a], Stuart H. Taylor [b,*]

[a] Departament d'Enginyeria Química, Universitat de València, C/Dr. Moliner 50, 46100 Burjassot, Valencia, Spain
[b] Cardiff University, School of Chemistry, Main Building, Park Place, Cardiff, South Glamorgan CF10 3AT, United Kingdom
[c] Instituto de Carboquímica (CSIC), C/Miguel Luesma 4, 50018 Zaragoza, Spain

ARTICLE INFO

Article history:
Received 14 January 2008
Received in revised form 27 March 2008
Accepted 28 March 2008
Available online 11 April 2008

Keywords:
Propane
Total oxidation
Nanocrystalline Co_3O_4
α-Al_2O_3
VOC
Alumina

ABSTRACT

Supported and unsupported nanocrystalline cobalt oxides have been shown to be extremely efficient catalysts for the total oxidation of propane. Total conversion with a high stability has been achieved at reaction temperatures as low as 250 °C. In the present work, a comparison between the catalytic performance of bulk and alumina-supported nanocrystalline cobalt oxide catalysts has been made. The influence of crystallite size, nature of the support (alpha, gamma and mesoporous alumina) and cobalt loading, has been probed. Unsupported cobalt oxide catalysts were more active than any supported cobalt oxide catalysts. The catalytic activity was mainly dependent on the crystallite size, decreasing with an increase in the crystallite size. Whilst the TOF of supported catalysts increases with both a decrease in the surface area of the support and an increase of the cobalt content. Only those catalysts with a cobalt content of 50 wt% achieve a catalytic activity per cobalt atom similar to that of unsupported Co_3O_4 prepared under similar conditions. High surface area alumina was shown to be a less efficient support especially at low Co-loadings due to the dispersion of cobalt on the surface leading to the formation of inactive Co–O–Al species. The low surface area support (α-Al_2O_3) presents a low capacity to isolate the cobalt oxide species resulting in a lower concentration of inactive Co–O–Al species and, therefore, the highest activity among supported catalysts. In conclusion, two parameters seem to determine the catalytic activity of nanocrystalline cobalt oxide: these are the presence of inactive Co–Al bonds (prevalent in supported catalysts) and also the size of the active Co_3O_4 particles.

1. Introduction

The release of volatile organic compounds (VOCs) to the atmosphere results in tangible environmental damage. For example, VOCs have been implicated in the formation of ground level ozone [1], ozone depletion [2] and often they act as greenhouse gases [3]. Amongst the number of methods employed to remove VOCs, catalytic oxidation is recognised as one of the most efficient as it provides the potential to destroy pollutants totally to carbon dioxide and water. VOCs are wide ranging in chemical functionality and their emission sources, but it is clear that linear short chain alkanes are some of the most difficult to destroy [4]. These compounds are emitted to the atmosphere in high concentrations, especially methane, which is the second most abundant greenhouse gas with a global warming potential ca. 20 times greater than CO_2. Another light alkane, propane, is also released to the atmosphere in increasing amounts since LPG (composed of primarily propane and butane) is ever more used as a substitute for gasoline and diesel in transport vehicles. A catalyst that completely removes propane, which is more difficult to eliminate than butane at low concentrations, is essential to reduce the impact on the environment [5]. Propane can also be emitted from stationary power sources.

Currently, the most active catalysts are those based on platinum and palladium, which are dispersed on a high surface area support. However, there still remains scope for improved catalysts as more active systems offer considerable economic advantages in terms of operating costs, and the level of environmental protection provided. An alternative to platinum group metal (PGM)-based catalysts, is the use of base-metal oxides. Unfortunately, the activity of these catalysts is in most cases lower. For the metal oxides, cobalt oxide has been shown to be one of the most efficient in the total oxidation of VOCs [6–8]. The use of cobalt oxide offers the advantage of both high reactivity and a relatively low price when compared with precious metals.

* Corresponding author.
E-mail addresses: benjamin.solsona@uv.es (B. Solsona), taylorsh@cardiff.ac.uk (S.H. Taylor).

0926-3373/$ – see front matter © 2008 Elsevier B.V. All rights reserved.
doi:10.1016/j.apcatb.2008.03.021

Studies have demonstrated that the addition of gold to cobalt-based catalysts significantly increases the activity for the total oxidation of short chain alkanes [9–12]. Other cobalt-containing catalysts [9,13–19] including perovskites [20–24] have also shown a high efficiency for combustion of light paraffins. However, one of the main disadvantages of using cobalt oxide as a catalyst is the low stability at high temperatures [25,26]. The most efficient cobalt oxide for VOC total oxidation is Co_3O_4 with a spinel structure, but at temperatures of ca. 700 °C the active phase Co_3O_4 transforms into the less active CoO, leading to a decrease in activity for VOC combustion [27]. A decrease of activity has also been observed without the $Co_3O_4 \rightarrow CoO$ transformation. The Co_3O_4 phase sinters and agglomerates, decreasing the activity with time online, without losing its structure at temperatures as low as 500 °C [28]. The addition of some promoters such as Nb has been shown to increase stability and prevent this sintering effect, although the reactivity is adversely affected [29].

Cobalt oxide catalysts are very efficient for the total oxidation of a large number of VOCs. However, no specific study has been carried out directly comparing the properties of bulk and supported catalysts. In the present work, a set of unsupported and alumina-supported cobalt oxide catalysts have been prepared, characterized and tested for the total oxidation of propane. Three different types of alumina have been used as support: α-Al_2O_3 (S_{BET} = 6 m^2/g), γ-Al_2O_3 (S_{BET} = 187 m^2/g) and a high surface area alumina (S_{BET} = 501 m^2/g). The latter alumina support is mesoporous, and this is the first study to report the activity of cobalt supported on a mesoporous alumina for total oxidation.

2. Experimental

2.1. Preparation of bulk cobalt oxide catalysts

The nomenclature and some characteristics of the catalysts are detailed in Table 1. CO-Commercial was used as supplied by Aldrich (Co_3O_4). CO-100 was prepared by dissolving cobalt(II) nitrate (Fluka, purity > 98%) in deionised water. This solution was evaporated, dried overnight at 120 °C and finally calcined in static air at 500 °C for 3 h. This sample was prepared in a similar way to that for the alumina-supported catalysts but without the addition of the support. CO-C1 and CO-C30 were prepared on a 5 g scale by grinding a mixture of cobalt(II) nitrate with ammonium hydrogen carbonate (molar ratio = 1:3) [30,31] in an agate mortar for 1 and 30 min, respectively. The solids were washed thoroughly with distilled water and collected by filtration, followed by drying for 16 h at 120 °C and calcined in static air for 3 h. Repeat preparations of the catalysts synthesised by the solid-state method were made and surface areas for the different batches were within experimental error of the BET method.

Table 1
Physico-chemical characteristics of cobalt containing catalysts

Catalyst	Co_3O_4 wt.% nominal	S_{BET} (m^2/g)	Particle size Co_3O_4 (nm)[a]	Catalytic activity[b]	
				T10	T50
α	0	6	–	–	–
α5	5	4	33.8	270	330
α20	20	4	42.4	230	280
α50	50	4	46.4	210	255
γ	0	187	–	–	–
γ5	5	182	6.4	310	380
γ20	20	156	12.8	295	360
γ50	50	74	42.4	215	255
HS	0	501	–	–	–
HS5	5	292	4.0	355	440
HS20	20	208	14.9	300	360
HS50	50	71	43.6	210	255
CO-100	100	14	45.2	205	235
CO-Commercial	100	2.0	70.6	265	335
CO-C1	100	14	38.0	200	230
CO-C30	100	99	15.5	175	205

[a] Estimated through the XRD patterns.
[b] Reaction temperature for propane conversions of 10 and 50%.

2.2. Preparation of alumina-supported cobalt oxide catalysts

Co supported on alumina catalysts was prepared by the wet impregnation method. Solutions of cobalt(II) nitrate were dissolved in water and added to the support. After stirring and heating at 80 °C the evaporation of water led to the formation of a paste. This paste was dried overnight at 120 °C and calcined in static air at 500 °C for 3 h. Supported alumina catalysts have been prepared with 5, 10, 20 and 50 wt% Co_3O_4 on three different alumina supports: (i) α-Al_2O_3 (Pechiney, S_{BET} = 6 m^2 g^{-1}), (ii) γ-Al_2O_3 (Sued-Chimie, S_{BET} = 187 m^2 g^{-1}) and (iii) high surface area alumina HS-Al_2O_3 (501 m^2/g) [32] where high surface area alumina was prepared as follows. Aluminium *sec*-butoxide, 1-propanol and stearic acid were employed as structure-directing agents. The preparation was carried out in a Teflon-lined stainless-steel autoclave at 100 °C for 48 h. The precursor was further heat treated in two steps: firstly, in N_2 at 410 °C for 4 h and subsequently in flowing air at 500 °C for 10 h [32].

2.3. Characterization techniques

Catalyst surface areas were determined by multi-point N_2 adsorption at 77 K. The data were treated in accordance with the BET method. Powder X-ray diffraction was used to identify the crystalline phases present in the catalysts. An Enraf Nonius FR590 sealed tube diffractometer, with a monochromatic Cu $K\alpha_1$ source operated at 40 kV and 30 mA was used. XRD patterns were calibrated against a silicon standard and phases were identified by matching experimental patterns to the JCPDS powder diffraction file.

Temperature-programmed reduction was performed using a micromeritics Autochem 2910 apparatus with a TCD detector. The reducing gas used was 10% H_2 in argon with a total flow rate of 50 ml min^{-1} (GHSV ca. 8000 h^{-1}). The temperature range explored was from room temperature to 900 °C with a heating rate of 10 °C min^{-1}.

Diffuse reflectance visible ultra violet spectroscopy (DR-UV–vis) was performed using a Cary 5 spectrometer equipped with a Praying Mantis attachment from Harric. The sample cell was equipped with a reaction chamber that allowed *in situ* experiments under a controlled environment. The samples were dehydrated in situ in dry air at 400 °C for 30 min. The spectra were collected after cooling to room temperature, and dry air was flowed through the sample to avoid rehydration. Infrared spectra were recorded at room temperature on a Nicolet 710 FTIR spectrometer. 5 mg of dried sample was mixed with 100 mg of dry KBr and pressed into a disk (600 kg/cm^{-2}), and data were collected in transmission mode. Scanning electron microscopy (SEM) was conducted on a Carl Zeiss EVO 40 microscope. All samples were dispersed on adhesive carbon discs and were uncoated.

2.4. Catalyst activity determination

Catalytic activity was measured using a fixed bed laboratory micro-reactor. For each experiment, 250 mg of powdered catalyst was placed in a 1/2″ o.d. quartz reactor tube. The reactor feed contained 8000 vppm propane in air with a total flow rate of

50 ml min^{-1}. The reactants and products were analysed by an online gas chromatograph with a thermal conductivity and a flame ionisation detector. Two chromatographic columns were employed: (i) Porapak Q (for CO_2 and hydrocarbons) and (ii) Molecular Sieve 5A (to separate O_2 and N_2). The temperature range 100–450 °C was explored and the reaction temperature was measured by a thermocouple placed in the catalyst bed. The differences between the inlet and outlet concentrations were used to calculate conversion data. In order to corroborate this data the chromatographic area of CO_2 was used as the comparative reference. These two ways lead us to adjust the carbon balance with an accuracy of ±2%. Analyses were made at each temperature until steady-state activity was attained (typically 40 min before the first analysis) and the results averaged. Blank experiments were conducted in an empty reactor which showed negligible activity over the temperature range used in this study.

3. Results

3.1. Characterization of catalysts

Table 1 shows the physico-chemical characteristics of cobalt-based catalysts. The commercial catalyst presented the lowest surface area, 2 $m^2 g^{-1}$. Depending on the preparation method, the surface areas of the bulk catalysts vary from 14 $m^2 g^{-1}$ to 99 $m^2 g^{-1}$. CO-100, the sample prepared as the supported catalysts but without employing the support, presented a surface area of 14 $m^2 g^{-1}$. CO-C1 and CO-C30 were prepared similarly only modifying the grinding time. It was observed that the longer the grinding time the higher the surface area obtained. In the case of CO-C30 a relatively high surface area of 99 $m^2 g^{-1}$ was obtained.

The surface area of supported catalysts depends on the support used and on the cobalt content. A drastic decrease in the surface area of mesoporous alumina-supported catalysts has been observed with increasing cobalt content. Thus for the catalysts with 5 wt% Co the surface area is 292 $m^2 g^{-1}$, whilst it is 71 $m^2 g^{-1}$ for the sample with a 50 wt% loading. In the case of α-Al_2O_3-supported catalysts the surface area is consistently lower than 10 $m^2 g^{-1}$.

Figs. 1 and 2 show the XRD patterns of unsupported and alumina-supported catalysts, respectively. The only pure cobalt phase identified was the spinel structured Co_3O_4 (JCPDS: 42-1467). No diffraction peaks related to a CoO phase were detected. The formation of a mixed Co–Al–O crystalline phase with a spinel structure ($CoAl_2O_4$) was also a distinct possibility in supported catalysts since it is almost indistinguishable from Co_3O_4 by XRD.

In the case of the bulk catalysts, Co_3O_4 was the only phase identified, whilst diffraction peaks corresponding to the support have also been detected for supported catalysts. The average crystallite size of Co_3O_4/$CoAl_2O_4$ was estimated using the full width half maximum of the characteristic diffraction peaks by applying the Scherrer equation. Thus, the average crystallite size

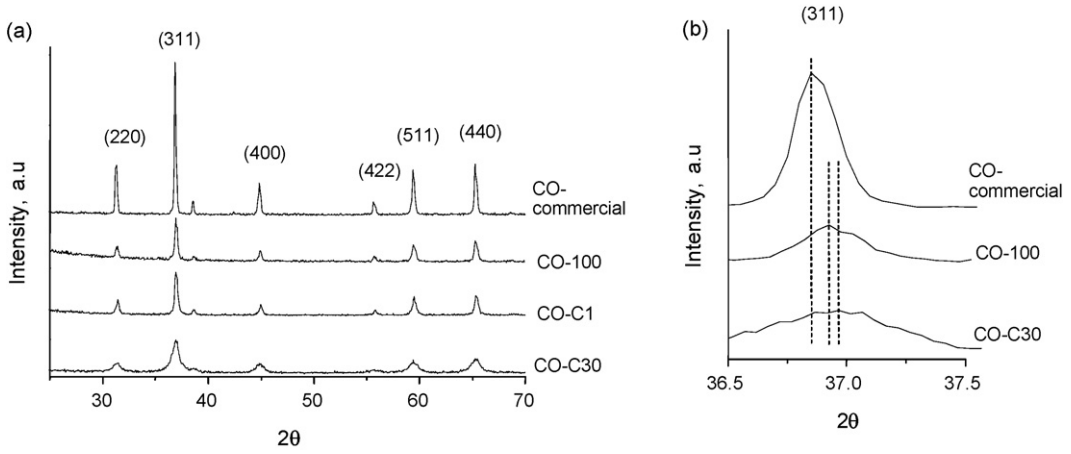

Fig. 1. XRD patterns of bulk cobalt oxide catalysts: (a) comparison of commercial cobalt oxide with catalysts prepared by solid-state method and (b) comparison of commercial, Co-C30 and Co-100 catalysts.

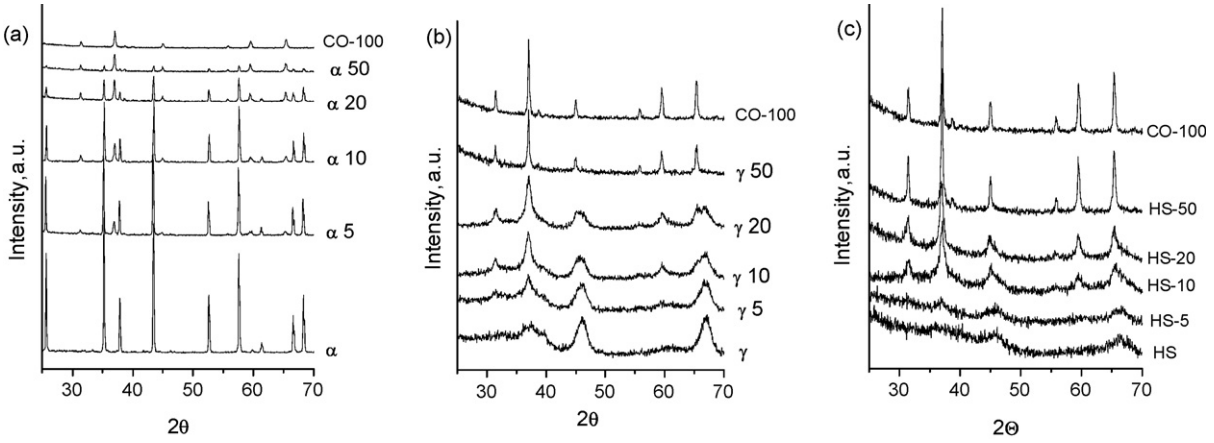

Fig. 2. Comparison of XRD patterns of alumina-supported cobalt oxide catalysts: supported on (a) α-Al_2O_3, (b) γ-Al_2O_3 and (c) high surface area mesoporous Al_2O_3.

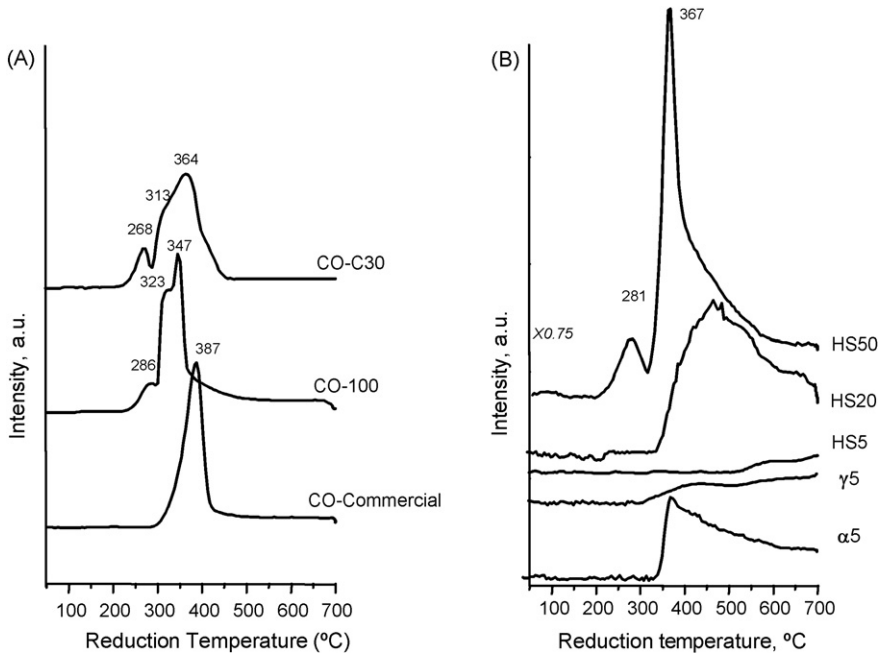

Fig. 3. TPR profiles of bulk and alumina-supported cobalt oxide catalysts: (A) bulk cobalt oxide and (B) alumina-supported cobalt oxide catalysts.

for mesoporous alumina-supported catalysts increased with increasing cobalt content (almost indistinguishable in the case of 5 wt% Co to ca. 44 nm for that of 50 wt% Co). In the case of Co/α-Al_2O_3 the crystallite size was relatively large, even for the catalyst with 5 wt% Co (ca. 34 nm) and increased with increasing Co loading.

For bulk Co_3O_4 catalysts, as expected, the crystallite size varied inversely to the surface area, from 70 nm in the case of the commercial catalyst to 15 nm for CO-C30. In addition, it has been observed that the commercial Co_3O_4 catalyst presents the diffraction peaks at lower angles, hence greater *d*-spacing, than the other bulk catalysts (especially CO-C30). This distortion of the unit cell has been related to a high number of defects in the Co_3O_4 spinel structure in the case of CO-C30 [33].

TPR experiments have also been conducted in order to estimate the reducibility of the catalysts. Fig. 3A shows the temperature-programmed reduction profiles for some representative bulk catalysts. Comparing the profile of the commercial Co_3O_4 to the CO-C30 catalyst, it can be appreciated that the reduction features appear at considerably lower temperatures for CO-C30. In addition, the profiles are very different. The major reduction feature for Co-C30 is considerably broader and shows evidence for another reduction peak within the main feature. Furthermore, Co-C30 shows a new lower temperature reduction peak, and this peak was not observed for the commercial sample.

In the case of CO-100 the reduction profile is similar to the one of CO-C30, although the reduction features are shifted to slightly higher temperatures. Some further subtle differences were apparent, as comparing Co-C30 with Co-100, the latter showed a smaller low temperature reduction peak and the main reduction feature was also less broad. Therefore we can conclude that the synthesis of high surface area cobalt oxide as CO-C30 favours the formation of more easily reducible sites. This is especially true if CO-C30 is compared to the commercial sample. The reduction of Co_3O_4 has been reported to proceed in two steps: (i) Co_3O_4 to CoO and (ii) CoO to Co [34]. According to the TPR experiments, it is clear that this reduction must involve some other intermediates, since three or four reduction bands can be clearly observed.

TPR profiles of alumina-supported catalysts have been plotted in Fig. 3B. Comparing the catalysts with 5 wt% cobalt oxide, important differences can be observed for the different supports employed. Thus, whilst α5 presented a high intensity reduction band at 364 °C, γ5 only showed a low intensity band at 360–370 °C, whilst HS5 consumed virtually no hydrogen in this temperature range. This reduction feature can be clearly associated with the presence of Co_3O_4 crystallites. In addition, a reduction peak with an onset at 600–700 °C was observed for catalysts supported on γ and HS-Al_2O_3. This reduction band at high temperature corresponds to cobalt oxide species, Co^{2+} and Co^{3+}, strongly bound to the support (surface Co–O–Al species reduced to Co metal) [35,36]. Jongsomjit et al. [37] reported that the Co–O–Al species formed in Co/Al_2O_3 catalysts presented a low degree of reducibility, lower than bulk Co_3O_4 crystallites and these Co–O–Al species are not identical to crystalline $CoAl_2O_4$ but they probably are surface compounds deficient in cobalt.

TPR of cobalt oxide catalysts supported on the high surface area alumina at different cobalt loadings are also reported in Fig. 3B. A broad band with the maximum at ca. 480 °C was observed for

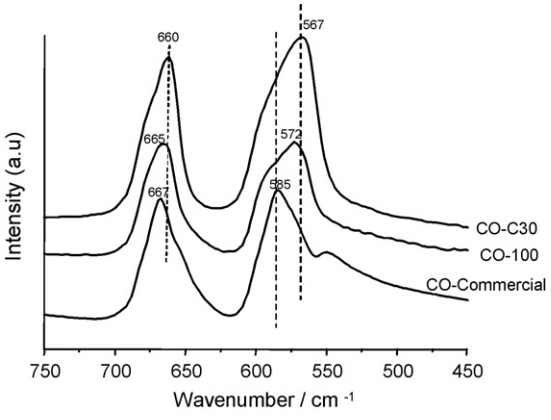

Fig. 4. FT-IR spectra of bulk cobalt oxide catalysts in the 750–450 cm^{-1} range.

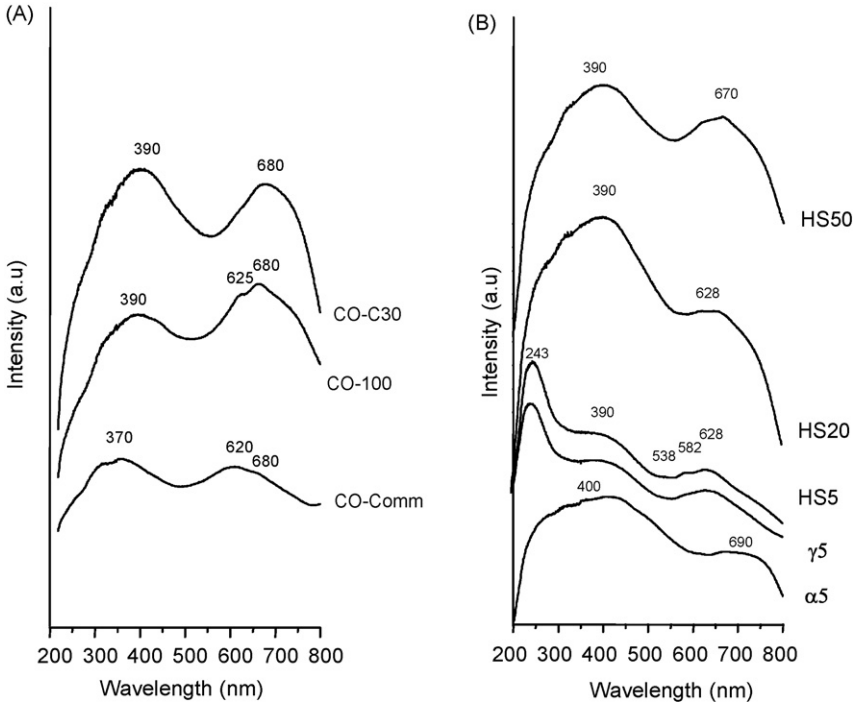

Fig. 5. DR-UV–vis spectra of bulk and alumina-supported cobalt oxide catalysts: (A) bulk cobalt oxide and (B) alumina-supported cobalt oxide catalysts.

HS20. In the case of HS50, the TPR profile was very similar to the bulk catalysts. According to the TPR data, the higher the Co-loading the greater the ease of reducibility of the cobalt species.

Catalysts were also studied by FT-IR. Catalysts with a cobalt content of 5 wt% presented spectra similar to the corresponding support (not shown here) and no bands associated with cobalt species could be observed. Therefore, FT-IR spectroscopy seemed to provide more useful information for bulk cobalt oxide catalysts. Fig. 4 shows the FT-IR spectra of some selected bulk catalysts. The absorption frequencies measured for the unsupported catalysts agree with those of the ν(Co–O) modes in the Co_3O_4 spinel structure [38], with bands at ca. 665 and 575 cm^{-1}. A shift to higher frequencies was observed with increasing the cobalt oxide crystallite size as indicated by the band at ca. 665 cm^{-1}. In

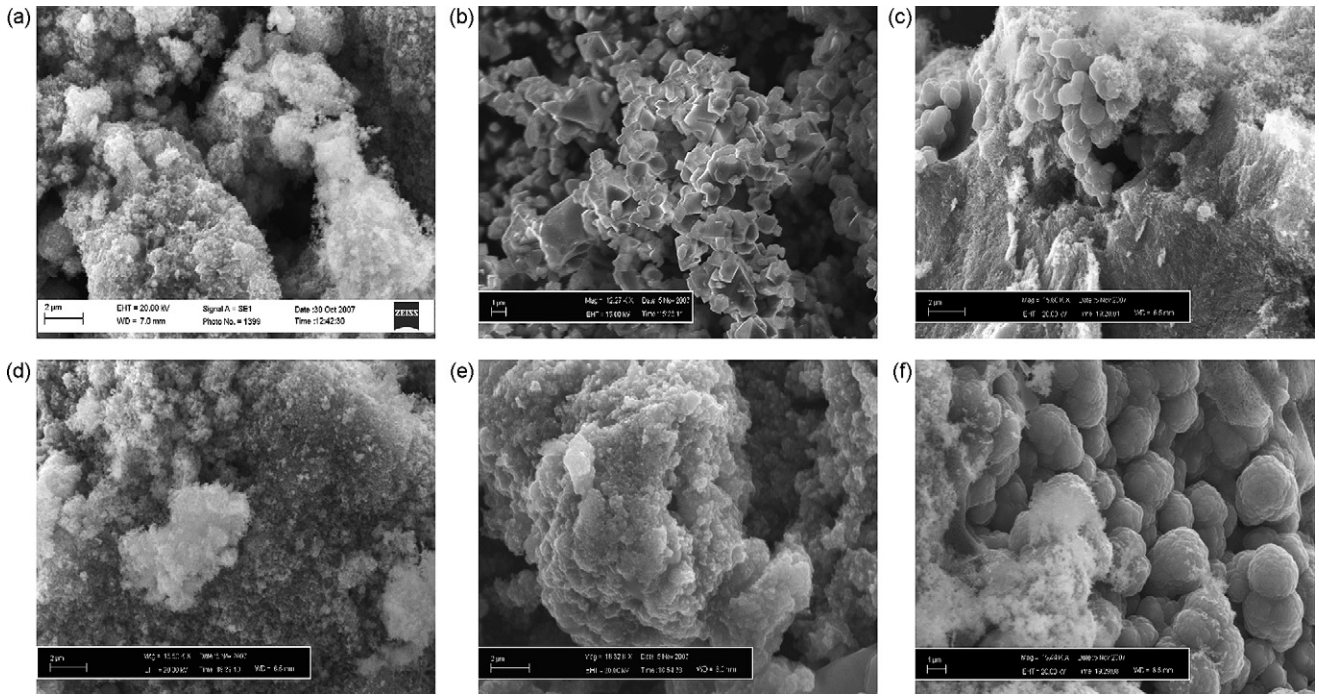

Fig. 6. Scanning electron microscopy secondary electron images of (a) fresh CO-C30, (b) fresh CO-Commercial, (b) fresh CO-100, (d) CO-C30 used in reaction at 225 °C for 30 h, (e) CO-C30 used in reaction at 475 °C for 30 h, and (f) CO-100 used in reaction at 475 °C for 30 h.

addition, the band at ca. 575 cm^{-1} appears to be the result of the overlap of two bands, one at ca. 568 cm^{-1} and another one at 585 cm^{-1}. Whilst the high surface area Co_3O_4 catalyst showed a maximum close to 568 cm^{-1}, in the case of the commercial catalyst, the peak maximum was close to 585 cm^{-1}. These shifts towards lower wavenumbers in CO-C30 indicate a decrease in the strength of the Co–O bond in Co_3O_4. The presence of other cobalt oxide species such as CoO, characterized by a broad band in the 400–550 cm^{-1} region [38,39], was not apparent in any of the unsupported catalysts.

Fig. 5 shows the DR-UV–vis spectra of some representative catalysts. Bulk catalysts present two broad bands at 370–390 and 625–680 nm, and these are related to the spinel Co_3O_4 structure with the Co ions in tetrahedral and octahedral coordination, respectively [28,40,41]. It can be observed that the relative intensity of both bands is different depending on the catalyst, although no clear correlation can be observed with respect to the surface area of the catalysts.

For supported catalysts with 5 wt% Co important spectral differences were observed (Fig. 5A). α5 presents spectra very similar to that of the bulk catalysts and is associated with the presence of Co_3O_4. In contrast, γ5 and HS5 present bands at 390 nm (related to Co_3O_4 in octahedral coordination) and two bands at 582 and 628 nm, which are associated with tetrahedral Co(II) species as in $CoAl_2O_4$ [28,40,41]. A band at 243 nm has been observed for γ5 and HS5, although the presence in the rest of the catalysts cannot be ruled out, due to the overlapping with the high intensity band at 370–390 nm. This band at 243 nm can be attributed to metal–ligand charge transfer [29].

SEM images of bulk catalysts with similar magnification are shown in Fig. 6. The morphology of the particles is significantly different depending on the preparation method employed. The fresh commercial Co_3O_4 (Fig. 6b) has distinct smooth square plates of varying sizes (from ca. 0.3 to 3 μm). In contrast, the catalyst prepared by a solid-state reaction (CO-C30) appears to be comprised of agglomerated nanoparticles with a spongy aspect (Fig. 6a). The agglomerated units of small particles had a diameter of approximately 200 nm. The catalyst prepared by precipitation (CO-100) was different to the other materials, with a number of differing morphologies (Fig. 6c). The catalyst appears to contain large particles upon which are a number of smooth semi-spherical clusters as well as the smaller nanosized clusters that were seen in CO-C30.

3.2. Activity of catalysts

The catalysts were tested for the oxidation of propane. For all the catalysts the main reaction product was CO_2, and in the case of supported catalysts no other products were observed. For the bulk Co_3O_4 catalysts traces of propylene were also observed at low propane conversions, and this is consistent with previous observations [30].

Fig. 7 shows the propane conversion achieved at different temperatures for the alumina-supported catalysts with different cobalt contents. It must be noted (not shown) that the aluminas employed as supports (α-Al_2O_3, γ-Al_2O_3, and HS-Al_2O_3) were largely inactive and the conversion was lower than 3% at the highest temperature studied (450 °C). The catalysts with higher cobalt content presented the highest catalytic activity. Although it also depended on the cobalt content, generally the most active supported catalysts were those on α-Al_2O_3, whereas those supported on HS-Al_2O_3 presented the lowest activity. Amongst the catalysts with a 5 wt% Co loading, cobalt supported on α-Al_2O_3 was the most active, whilst cobalt supported on high surface area alumina presented the lowest conversion. A similar trend was

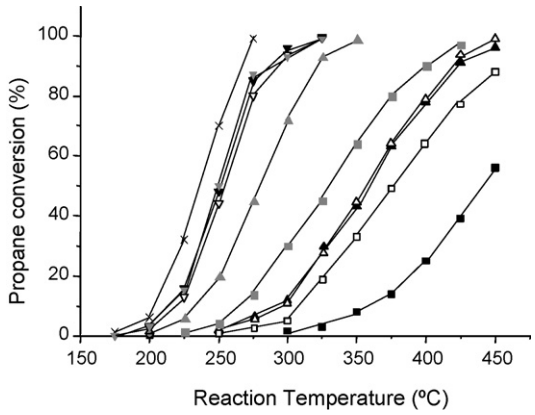

Fig. 7. Propane conversion as a function of temperature over alumina-supported cobalt oxide catalysts. Reaction conditions detailed in text. Symbols: (■) HS5, (▲) HS20, (▼) HS50, (□) γ5, (Δ) γ20, (V) γ50, (■) α5, (▲) α 20,(▼) α 50, (×) CO-100.

observed for the catalysts with 20 wt% Co, although to a lesser degree. In contrast, if the activity of catalysts with 50 wt% Co oxide was compared, no appreciable differences were observed for the different supports employed.

The trends in activity for the supported catalysts can be summarised by considering the temperatures required for 10 and 50% propane conversion (T10 and T50). These data are presented in Table 1. In general, T10 and T50 increased as the surface area of the catalyst support increased. Furthermore, for all of the supported catalysts T10 and T50 decreased as the loading of cobalt was increased on each support.

The activity of the different bulk Co_3O_4 catalysts is shown in Fig. 8. The commercial catalyst CO-Commercial was the least active and CO-C30 showed the highest activity, achieving a conversion higher than 99% at only 250 °C. In short, it was observed that the higher the surface area (and the lower the particle size) the greater the catalytic activity. These trends are reinforced by consideration of the trends of T10 and T50 for the unsupported catalysts (Table 1).

Except in the case of the commercial sample, bulk Co_3O_4 catalysts are remarkably more active than alumina-supported catalysts. Generally, the catalytic activity in the present work follows the order:

Bulk Co_3O_4 > Co/α-Al_2O_3 > Co/γ-Al_2O_3 > Co/HS-Al_2O_3 > α-Al_2O_3, γ-Al_2O_3, HS-Al_2O_3

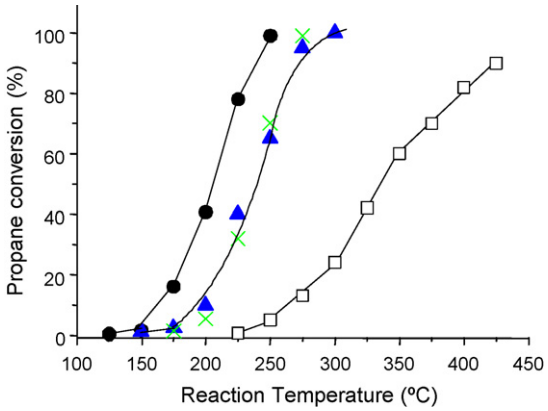

Fig. 8. Variation of the propane conversion with the reaction temperature over bulk cobalt oxide catalysts. Reaction conditions detailed in text. Catalysts: (●) CO-C30, (▲) CO-C1, (×) CO-100, (□) CO-Commercial.

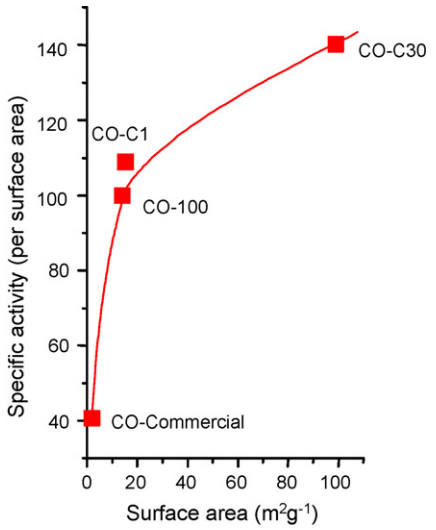

Fig. 9. Influence of the surface area on the specific activity (catalytic activity normalized per unit surface area) over bulk cobalt oxide catalysts. *Notes*: (i) CO-100 has been taken as a reference (specific activity = 100) and (ii) catalytic activity calculated at a reaction temperature = 175 °C.

4. Discussion

4.1. Catalytic performance of bulk Co_3O_4

Bulk cobalt oxide catalysts present higher catalytic activity than those supported on alumina. The exceptional performance of CO-C30 should be highlighted as it achieves ca. 100% conversion at only 250 °C. This value is remarkably lower than other results published in the literature [7]. Conversely, the Co_3O_4 from a commercial supplier, CO-Commercial, presents the lowest activity. For unsupported catalysts there was a direct correlation between surface area and propane total oxidation activity and an inverse relationship with increasing crystallite size. However, the relationship between the surface area normalised rate of oxidation (specific activity) and the surface area is not linear (Fig. 9). The specific activity increases as the surface area increases and therefore more complex factors, rather than the total catalyst surface area, must influence the exceptionally high activity of CO-C30. It seems that the small size of the crystallites may give rise to new and/or more easily accessible active sites, which are not present in the more highly crystalline Co_3O_4 catalysts [7]. The specific nature of the active sites responsible for total oxidation is still unclear; however, the catalytic activity during the deep oxidation of short chain alkanes has been related to the reducibility of the active sites of the catalyst [42]. Busca and co-workers demonstrated that for a Co_3O_4 catalyst lattice O^{2-} anions (nucleophilic oxygen species) were those involved in propane catalytic total oxidation [42]. Therefore, the reaction occurs through a Mars Van Krevelen mechanism involving lattice oxygen via a redox cycle. Accordingly, Bahlawaue [43] also demonstrated that the combustion of methane follows a Mars Van Krevelen mechanism, which depends on the fast migration of oxygen ions through the lattice of the cobalt oxide.

Consequently the reducibility of the catalyst is an important factor for the reactivity [6]. It has been shown that the reduction peaks in the TPR profiles of CO-C30 are present at temperatures lower than those of the commercial Co_3O_4 material (Fig. 3). If the reducibility of CO-C30 is compared to that of CO-100 the trend is not so clear, although the species that appear at low temperatures are more easily reduced in the case of CO-C30. Furthermore, vibrational spectroscopy results confirmed that the strength of the Co–O bond from the Co_3O_4 phase was weaker in the catalysts with the smallest crystallite size and, therefore, the reducibility of Co_3O_4 increases as the crystallite size decreases. The small crystallite size of CO-C30, when compared with more highly crystalline catalysts, results in cobalt oxide species with particular characteristics, i.e. (i) a greater number of low coordination defect lattice oxygen sites (XRD data); (ii) a lower Co–O bond energy in the highly crystalline Co_3O_4 phase (FT-IR data) and (iii) a higher reducibility of the cobalt oxide species, especially those species that can be reduced at low temperatures. These factors contribute to the high activity of the Co_3O_4 with a nanocrystalline structure.

4.2. Catalytic performance of supported cobalt catalysts

All three alumina supports are relatively inactive for the combustion of propane in the range of temperatures studied, and it is clear that the activity is almost exclusively due to the presence of cobalt. The propane conversion achieved over Co/alumina catalysts clearly increased with the cobalt content, regardless of the nature of the support. However, the increasing activity is not only due to the higher number of cobalt sites but it is also related to their different nature. Thus, it can also be observed that the activity per cobalt atom increases with the cobalt loading. By increasing the cobalt loading the cobalt oxide crystallite particle size increases (see Table 1) as well as the reducibility. According to this, as previously reported by other authors [44–46] for supported cobalt oxide catalysts, large Co_3O_4 particles are more easily reduced than small Co_3O_4 particles. Therefore the higher reactivity of catalysts with high cobalt content must be related to the high reducibility of large Co_3O_4 particles.

In the present work, it has also been observed that the nature of the support affects the crystallite size since low surface area supports promote the agglomeration of cobalt particles as larger Co_3O_4 crystals (see Table 1). Therefore the use of supports with low surface area leads to an increase of the cobalt oxide particle size, increasing their reducibility and enhancing the catalytic activity of the cobalt-supported catalysts.

The differences in activity for catalysts with 5 wt% Co provide an important comparison for understanding the performance of cobalt-supported catalysts in the total oxidation of propane (Fig. 7). HS5 presents an extremely low activity (T50 = 440 °C) meanwhile α5 was the most active catalyst (T50 = 330 °C). The catalysts supported on γ-Al_2O_3 showed an intermediate activity (T50 = 380 °C).

In contrast to this, the catalytic activity results of catalysts with 50 wt% Co on different supports presents minimal variation. This must be related to (i) the high cobalt content that exceeds the capacity of coverage of any support, and therefore most of the cobalt is present as large three-dimensional Co_3O_4 crystallites and; (ii) the similar crystallite size of the Co_3O_4 crystals for the different alumina supports.

Inspection of the DR-UV–vis spectra can help to explain the behaviour of Co/alumina catalysts. Two different types of bands have been observed, one type at ca. 390 and 680 nm, related to the spinel structure of Co_3O_4 and, the second type at 538, 582 and 628 nm, which relate to dispersed tetrahedral Co–O–Al species, similar to $CoAl_2O_4$ spinel species. The relative intensity of these Co–O–Al bonds decreased with the increasing the cobalt oxide particle size, and it takes place when increasing cobalt loading or decreasing the surface area of the support. Taking into account that the $CoAl_2O_4$ spinel phase has been reported to be relatively inactive for the oxidation of short chain alkanes [41], the low activity of supported catalysts with low Co_3O_4 particle size must be related to the higher amount of inactive Co–O–Al species. Similarly to that observed here, Jalama et al. [47] and Sun et al. [48] have reported,

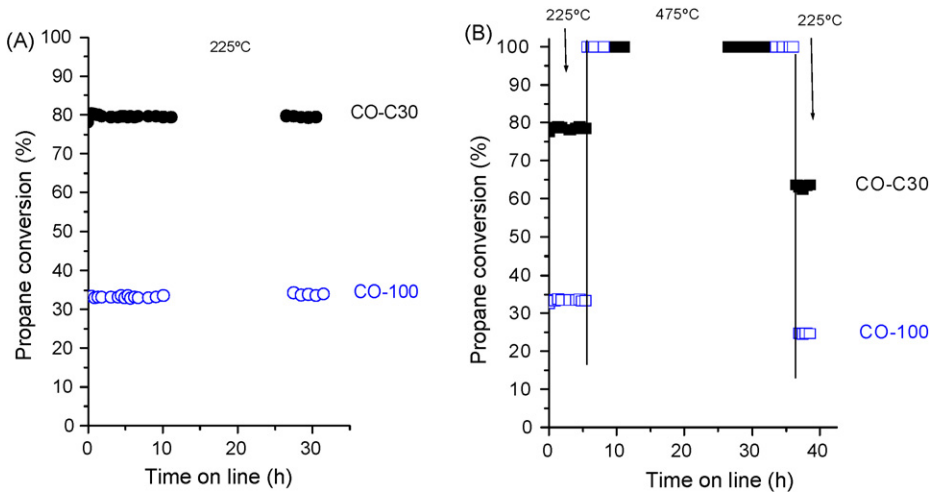

Fig. 10. Study of the stability of CO-C30 (●,■) and CO-100 (○,□) catalysts. Variation of the propane conversion with the time: (A) (●,○) 30 h online at 225 °C and (B) (■,□) 5 h at 225 °C + 30 h at 475 °C + 2 h at 225 °C. Reaction conditions detailed in text.

for the Fischer–Tropsch reaction, that highly dispersed Co-species lead to a lower activity and further demonstrates the importance of the state of the cobalt for activity.

4.3. Comments on the catalytic performance of cobalt oxide-based catalysts

As previously known, and further corroborated in this work, cobalt oxide-based catalysts are highly efficient for short chain alkane combustion. It must also be highlighted that according to our results, unsupported Co_3O_4 catalysts present a catalytic activity higher than catalysts of Co_3O_4 supported on a range of aluminas. Amongst the bulk catalysts, the most active was the one with the highest surface area and the lowest crystallite size (CO-C30). Amongst alumina-supported catalysts, cobalt catalysts supported on the lowest surface area support (α-Al_2O_3) were the most active catalysts.

Regarding the relationship between the Co_3O_4 particle size and the catalytic activity a completely different trend was observed between unsupported and supported catalysts. A decrease of activity with increasing crystallite size has been observed for the unsupported catalysts, whereas an increase of activity was found for the supported catalysts. In the case of bulk catalysts small crystallites lead to the formation of new and easily reducible highly active catalysts. In contrast, for supported catalysts the formation of low reducible Co–O–Al species are favoured in catalysts with low Co_3O_4 particle size.

It is also worth commenting on the stability of the bulk catalysts employed. Trigueiro et al. [29] have reported that Co_3O_4 deactivates in the oxidation of methane at 500 °C, decreasing in activity from 75 to 68% after just 7 h online. As mentioned previously, some other studies have observed similar unstable behaviour with cobalt oxide-based catalysts. Short chain alkanes are less reactive compared to other hydrocarbons, such as olefins, alcohols, ketones, etc. [49]. Within the alkanes, it is known that the reactivity decreases with decreasing chain length, with methane being the least reactive. In the present work we have used propane as the substrate, which is more reactive than methane. Due to the high reactivity of cobalt-based catalysts, lower temperatures can be used to achieve total conversion. In a similar recent study to the present one, it has been demonstrated that a nanocrystalline Co_3O_4 shows stable conversion after eight cycles from room temperature to the temperature of full conversion [7]. Therefore, the increased activity of these cobalt catalysts means that excessively high reaction temperatures are not required, resulting in a relatively stable catalyst. To check these assumptions new experiments were undertaken. In the present work the most active catalyst CO-C30 presents a stable propane conversion = 80% after 30 h online at 225 °C (Fig. 10, full circles). In order to test the stability of the catalyst at high temperatures, we studied the catalytic performance of CO-C30 at 475 °C (Fig. 10, full squares). Due to the high reactivity of this catalyst, our experimental set-up does not permit us to work at space velocities high enough to give propane conversion lower than 100% at a reaction temperature as high as 475 °C. Therefore in order to probe potential deactivation, catalytic activity was measured at 225 °C. After 5 h online at 225 °C (stable conversion *ca.* 80%) the temperature was increased to 475 °C and monitored for 30 h. After the 30-h period the temperature was reduced to 225 °C, and propane conversion determined. Using this procedure, it was evident that deactivation had occurred as the conversion was reduced to 60–65%, compared with ca. 80% for the fresh catalyst. The stability of another representative bulk cobalt oxide catalyst, CO-100, was also studied in a similar way at 225 °C (Fig. 10, open circles) and 475 °C (open squares). The propane conversion remained stable

Table 2
Influence of the catalytic use on the Co_3O_4 particle size over some selected bulk catalysts

Catalyst	Particle size[a]			Loss of activity[b]	
	Fresh	After 30 h/225 °C	After 30 h/475 °C	After 30 h/225 °C	After 30 h/475 °C
CO-100	45.2	Not determined	54.7	−1.9	23.6
CO-C30	15.5	17.9	25.6	1.2	21.5

[a] Particle size (average) estimated through the XRD pattern using the Scherrer equation.
[b] Loss of activity as (conversion at 225 °C of fresh catalyst − conversion at 225 °C of used catalyst)/(conversion at 225 °C of fresh catalyst) × 100.

(ca. 34%) for 30 h at 225 °C. The summary in Table 2 shows a small negative value for the loss of activity, and this corresponds to a slight increase of conversion from 33.8% to 34.5% after 30 h. This increase was not significant and is within experimental error. When the catalyst was operated at 475 °C for 30 h a similar deactivation was also observed as conversion was reduced from the initial level of 33% to 25%.

Table 2 shows the average crystallite size of CO-C30 and CO-100 catalysts before and after the stability tests. The crystallite size of fresh CO-C30 was 15.5 nm and after 30 h online at 225 °C the cobalt oxide crystallite size increased slightly to 17.9 nm. In spite of the higher crystallinity, no major difference in the catalytic conversion was observed. According to the SEM study the use of CO-C30 at 225 °C (Fig. 6d) had no noticeable effect on the apparent particle size or morphology, maintaining the spongy aspect of the fresh catalysts. In contrast, after 30 h online at 475 °C the crystallite size was found to increase significantly (25.6 nm) and may well explain the significant decrease of the catalytic activity. In fact, as observed in the SEM image (Fig. 6e), use at 475 °C resulted in sintering of the material and a loss of the finer clustered material.

Similarly the crystallite sizes for fresh and used CO-100, tested at 475 °C, were 45.2 and 54.7 nm, respectively. According to SEM, CO-100 used at 475 °C (Fig. 6f) resulted in a change of the surface structure of the semi-spherical particles which take on a "cauliflower" appearance. The small clusters apparent in the fresh catalyst are still present but now in a lower quantity.

5. Conclusions

A nanocrystalline cobalt oxide catalyst with high surface area (99 m^2/g) has been shown to be extremely active for the total oxidation of propane. In fact, total conversion has been attained at a reaction temperature as low as 250 °C. Bulk Co_3O_4 catalysts have shown higher activity than the supported catalysts for the total oxidation of propane. For bulk catalysts, those with the highest surface area were the most reactive. In addition, this catalyst also presented the highest specific activity (normalised for the surface area) indicating that the activity did not scale linearly with surface area. High surface area Co_3O_4 was more easily reduced, with a low Co–O bond strength and higher defect concentration.

The cobalt catalysts supported on the high surface area alumina presented the lowest activity from all supported catalysts. The high capacity of the high surface area alumina to disperse the cobalt oxide on the surface leads to a high amount of dispersed Co–Al species with low reducibility and therefore with low activity. In contrast the α-alumina was shown to be the most favourable support. The α-alumina, which presents an extremely low surface area, has less of an influence on the active cobalt oxide catalyst component, which behaves more like bulk Co_3O_4.

The bulk Co_3O_4 catalysts were stable under the conditions used for propane oxidation. The stability is due to the relatively low reaction temperatures that can be used for propane oxidation. However, studies using the catalysts at much greater temperatures than those required for 100% propane conversion demonstrate that bulk Co_3O_4 catalysts may partially deactivate with time-on-stream.

Acknowledgements

S. Taylor would like to thank Cardiff University, School of Chemistry, for funding. B. Solsona would like to thank the Spanish MEC for his RyC contract.

References

[1] B.J. Finlayson-Pitts, J.N. Pitts, Science 276 (1997) 1045.
[2] M.J. Molina, F.S. Rowland, Nature 249 (1974) 810.
[3] H. Rodhe, Science 248 (1990) 1217–1219.
[4] T.V. Choudhary, S. Banerjee, V.R. Choudhary, Appl. Catal. A: Gen. 234 (2002) 1.
[5] V.R. Choudhary, G.M. Deshmukh, Chem. Eng. Sci. 60 (2005) 1575.
[6] G. Busca, M. Daturi, E. Finocchio, V. Lorenzelli, G. Ramis, R.J. Willey, Catal. Today 33 (1997) 239.
[7] B. Solsona, I. Vázquez, T. García, T.E. Davies, S.H. Taylor, Catal. Lett. 116 (2007) 116.
[8] J.G. McCarthy, Y.F. Chang, V.L. Wong, M.E. Johansson, Preprints ACS Div. Petr. Chem. 42 (1997) 158.
[9] A.C. Gluhoi, N. Bogdanchikova, B.E. Nieuwenhuys, Catal. Today 113 (2006) 178.
[10] R.D. Waters, J.J. Weimer, J.E. Smith, Catal. Lett. 30 (1995) 181.
[11] M. Haruta, Now Future 7 (1992) 13.
[12] B.E. Solsona, T. García, C.D. Jones, S.H. Taylor, A.F. Carley, G.J. Hutchings, Appl. Catal. A: Gen. 312 (2006) 67.
[13] I. Yuranov, N. Dunand, L. Kivi-Minsker, A. Renken, Appl. Catal. B: Environ. 36 (2002) 183.
[14] N.A. Merino, B.P. Barbero, P. Grange, L.E. Cadus, J. Catal. 231 (2005) 232.
[15] V.R. Choudhary, G.M. Deshmukh, S.G. Pataskar, Environ. Sci. Technol. 39 (2005) 2364.
[16] S.F. Ji, T.C. Xiao, H.T. Wang, E. Flahaut, K.S. Coleman, M.L.H. Green, Catal. Lett. 75 (2001) 65.
[17] V.G. Milt, E.A. Lombardo, M.A. Ulla, Appl. Catal. B: Environ. 37 (2002) 63.
[18] L.F. Liotta, G. Di Carlo, G. Pantaleo, G. Deganello, Catal. Commun. 6 (5) (2005) 329.
[19] V.R. Choudhary, B.S. Uphade, S.G. Pataskar, A. Keshavaraja, Angew. Chem., Int. Ed. 35 (20) (1996) 2393.
[20] V.R. Choudhary, S. Banerjee, S.G. Pataskar, Appl. Catal. A: Gen. 253 (2003) 65.
[21] B. Kucharczyk, W. Tylus, Catal. Today 90 (2004) 121.
[22] N. Yi, Y. Cao, Y. Su, W.L. Dai, H.Y. He, K.N. Fan, J. Catal. 230 (2005) 249.
[23] V. Szabo, M. Bassir, A. Van Neste, S. Kaliaguine, Appl. Catal. B: Environ. 43 (2003) 81.
[24] V.R. Choudhary, B.S. Uphade, S.G. Pataskar, G.A. Thite, Chem. Commun. (9) (1996) 1021.
[25] M.F.M. Zwinkels, S.G. Jaras, P.G. Menon, T.A. Griffin, Catal. Rev. Sci. Eng. 35 (1993) 319.
[26] A.Yu. Khodakov, J. Lynch, D. Bazin, B. Rebours, N. Zanier, B. Moisson, P. Chaumette, J. Catal. 168 (1997) 16.
[27] L.F. Liotta, G. Di Carlo, G. Pantaleo, A.M. Venezia, G. Deganello, Appl. Catal. B: Environ. 66 (2006) 217.
[28] D.L. Trimm, Catal. Today 26 (1995) 231.
[29] F.E. Trigueiro, C.M. Ferreira, J.-C. Volta, W.A. Gonzalez, P.G. Pries de Oliveria, Catal. Today 118 (2006) 425.
[30] T. Davies, T. Garcia, B. Solsona, S.H. Taylor, Chem. Commun. 32 (2006) 3417.
[31] H. Yang, Y. Hu, X. Zhang, G. Qiu, Mater. Lett. 58 (2004) 387.
[32] (a) F. Vaudry, S. Khodabandeh, M.E. Davis, Chem. Mater. 8 (1996) 1451; (b) L. Kaluza, M. Zdrazil, N. Zilkova, J. Cejka, Catal. Commun. 3 (4) (2002) 151.
[33] U. Zavyalova, P. Scholz, B. Ondruschka, Appl. A: Gen. 323 (2007) 226.
[34] A.R. Belambe, R. Oukaci, J.G. Goodwin Jr., J. Catal. 166 (1997) 8.
[35] A. Sirijaruphan, A. Horvath, J.G. Goodwin Jr., R. Oukaci, Catal. Lett. 91 (2003) 89.
[36] P. Arnoldy, J.A. Moulijn, J. Catal. 93 (1985) 38.
[37] B. Jongsomjit, J. Panpranot, J.G. Goodwin, J. Catal. 2044 (2001) 98.
[38] G. Busca, R. Guidetti, V. Lorenzelli, J. Chem. Soc., Faraday Trans. 86 (1990) 989.
[39] Z.T. Fattakhova, A.A. Ukharskii, P.A. Shiryaev, A.D. Berman, Kinet. Katal. 27 (1986) 884.
[40] J.Y. Yan, M.C. Kung, W.M.H. Sachtler, H.H. Kung, J. Catal. 172 (1997) 178.
[41] L.F. Liotta, G. Pantaleo, A. Macaluso, G. Di Carlo, G. Deganello, Appl. Catal. A: Gen. 245 (2003) 167.
[42] E. Finocchio, G. Busca, V. Lorenzelli, V. Sanchez Escribano, J. Chem., Faraday Trans. 92 (1996) 1587.
[43] N. Bahlawaue, Appl. Catal. B: Environ. 67 (2006) 168.
[44] J.S. Girardon, A.S. Lermontov, L. Gengembre, P.A. Chernavskii, A. Griboval-Constant, A.Y. Khodakov, J. Catal. 230 (2005) 339.
[45] L.R. Bechara, D. Balloy, J.Y. Dauphin, J. Grimblot, Chem. Mater. 11 (1999) 1703.
[46] D.G. Castner, P.R. Watson, I.Y. Chan, J. Phys. Chem. 94 (1990) 819.
[47] K. Jalama, N.J. Coville, D. Hildebrandt, D. Glasser, L.L. Jewell, Appl. Catal. A: Gen. 326 (2007) 164.
[48] S. Sun, N. Tsubaki, K. Fujimoto, Appl. Catal. A: Gen. 202 (2000) 121.
[49] T. Blasco, J.M. López Nieto, Appl. Catal. A: Gen. 157 (1997) 117.